# Higgs boson decay constraints on a model with a universal extra dimension

Anindya Datta,[1,*] Ayon Patra,[2,†] and Sreerup Raychaudhuri[3,‡]

[1]*Department of Physics, University of Calcutta, 92 Acharya Prafulla Chandra Road,
Kolkata 700009, India*
[2]*Department of Physics, Oklahoma State University, Stillwater, Oklahoma 74078, USA*
[3]*Department of Theoretical Physics, Tata Institute of Fundamental Research,
1 Homi Bhabha Road, Mumbai 400005, India*

We investigate the impact of the latest data on Higgs boson branching ratios on the minimal model with a universal extra dimension. Combining constraints from vacuum stability requirements with these branching ratio measurements we are able to make realistic predictions for the signal strengths in this model. We use these to find a lower bound of 1.3 TeV on the size parameter $R^{-1}$ of the model at 95% confidence level, which is far more stringent than any other terrestrial bound obtained till now and is compatible with the dark matter constraints from the Wilkinson Microwave Anisotropy Probe data.

The discovery of the 125–126 GeV Higgs boson—or its close lookalike—at CERN, Geneva, in the previous year [1], has proved to be a game-changing moment in phenomenological studies of electroweak interactions. Gone are speculations about Higgsless models [2], strongly coupled Higgs sectors [3] and fears that the Higgs boson self-coupling may hit a Landau pole at some large energy scale [4]. Instead, today's theoretical studies have other concerns, such as stability of the electroweak vacuum, fine-tuning constraints and the requirement that the measured Higgs boson mass and branching ratios be correctly explained in whatever model happens to be the subject of the study. At the present instance, there is no compelling reason, beyond certain theoretical prejudices (like grand unification), to believe that we require anything other than the Standard Model (SM) to explain all the known phenomena on a terrestrial scale. Destabilization of the SM vacuum at some energy scale below the Planck scale could be one of the strongest hints of new physics [5], but at the moment this issue is mired in uncertainties of the top quark mass measurement [6].

Nevertheless, we do require physics beyond the Standard Model, and this requirement arises as soon as we look outside the confines of our Earth into the cosmos beyond. Here it is well known that the SM fails to provide explanations for (i) the composition of dark matter [7], (ii) the nature of dark energy [8] and (iii) the amount of $CP$ violation required for baryogenesis [9]. Of these, perhaps the most tractable problem is the first one, viz. the generation of a model for dark matter, for all that is required is a model for a stable, weakly interacting massive particle (WIMP). The most famous model which provides

this is, of course, supersymmetry with conservation of $R$ parity, where the lightest supersymmetric particle is the WIMP in question [10]. An alternative model, which was proposed about a decade ago, is one with a so-called universal extra dimension [11]. In the minimal model of this kind (mUED), each five-dimensional SM field is replaced by a tower of Kaluza-Klein (KK) modes, each labeled by a KK number $n$ and having masses given (at tree level) by $M_n = (M_0^2 + n^2 R^{-2})^{1/2}$. Here, the lightest of the $n = 1$ particles is stable and weakly interacting due to a $Z_2$ symmetry called KK parity, defined in terms of KK number by $(-1)^n$. This lightest KK particle, called the LKP, is an excellent candidate for dark matter [12].

At a high energy collider, the behavior of the mUED models is very similar to that of supersymmetric models [13]. The $n = 1$ states form analogues of the supersymmetric particles, exhibiting cascade decays ending in the LKP, which is then a source of missing energy and momentum. A major difference from supersymmetry is the presence of $n = 2$ and higher KK modes, which could perhaps be produced as resonances in a high energy machine like the LHC [14]. However, a more significant difference arises when we consider the ultraviolet behavior of the mUED model (or any model with KK modes), as was pointed out in a pioneering paper by Dienes, Dudas, and Gherghetta [15]. This is the fact that when we allow the SM coupling constants to run in this model, we encounter repeated KK thresholds at every scale $n/R$, so that, when considered over a large range of energies, the coupling constant exhibits a piecewise logarithmic running closely mimicking a power law dependence. As a result, it has been shown that (a) the electromagnetic coupling hits a Landau pole at as low a scale as $\Lambda \approx 40R^{-1}$, and (b) there is approximate (but not exact) unification of the three gauge coupling constants at an even lower scale $\Lambda \approx 20R^{-1}$. One therefore assumes that the low energy theory has a cutoff at

*adphys@caluniv.ac.in
†ayon@okstate.edu
‡sreerup@theory.tifr.res.in

either of these values, and phenomenological studies are made accordingly. This has been the standard practice in mUED studies over the past decade.

Of course, it is not only the gauge couplings that run faster in this model, but also the scalar self-coupling $\lambda$. It has been shown [16] that if the self-coupling $\lambda = M_H^2/2v^2$ is less than 0.18 at the electroweak scale, then its renormalization group evolution will inexorably drive it to zero at some high scale, at which point the electroweak vacuum will become unstable. Taking the experimental range 122 GeV $\leq M_H \leq$ 127 GeV for the Higgs boson mass, we obtain $0.123 \leq \lambda \leq 0.133$, which is clearly below 0.180. It follows that the electroweak vacuum in this model will indeed destabilize at some high scale, as, in fact, happens in the Standard Model itself at very high scales. The surprise lies in that fact that the "power law" running of $\lambda$ in the mUED model is so fast that the destabilization takes place at a scale which is always below $6R^{-1}$. At this surprisingly low scale, new physics must come to the rescue, and hence the destabilization scale can be treated as a cutoff for the mUED model.

The exact value of the cutoff scale is determined by evaluating the running coupling constant $\lambda$ and determining where it vanishes [16]. The most important input parameters which determine this running are the mass of the Higgs boson ($M_H$) and the size parameter ($R^{-1}$), which is nothing but the inverse of the compactification radius of the extra dimension. The solid (red) lines in Fig. 1 show the variation of the cutoff scale $\Lambda$, in units of $R^{-1}$, as a function of this size parameter $R^{-1}$, for two values of Higgs boson mass $M_H = 122$, 127 GeV (which represent the $3\sigma$ experimental limits). The (red) hatching, therefore, represents all the intermediate values of $M_H$. Horizontal (blue) lines represent the different KK levels $n/R$, for
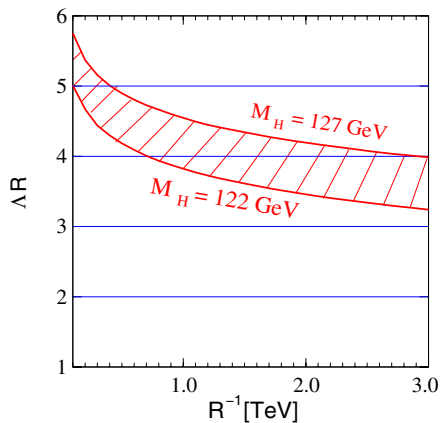
$n = 1, 2, ..., 6$. Our results shown here correspond closely to similar results shown in Ref. [17].

Obviously, assuming tree-level masses, the number of KK modes with mass $M_n \approx n/R$ which can participate in any process will be given by the nearest integer lower than the solid (red) curve for a given value of $R^{-1}$. It is clear that this number can only vary between 3 and 5, and can never reach higher values such as 20 and 40 which used to be assumed earlier. Note that in generating Fig. 1, and subsequently, we have fixed the top quark mass at $m_t = 172.3$ GeV. Variation of the top quark mass between its experimentally allowed limits [18] does result in some distortion of the curves, as the related Yukawa coupling plays a role in the running of the self-coupling $\lambda$. However, these distortions have very minor effects on the final conclusions of this article, and hence are not shown here.

In an earlier article [23], written at a stage when the new boson discovered at the CERN LHC had not yet been identified with any certainty as the Higgs boson, two of the present authors had shown that this low value of cutoff (i.e. small number of KK modes to sum over) leads to a compressed spectrum of KK modes of SM fields at any level $n \geq 1$, which presents serious difficulties for detection at the Tevatron and LHC. However, it was not possible to impose constraints on the model from the Higgs boson decay branching ratios, which were very imperfectly measured [1] at that stage. Now, however, we have better experimental results on these branching ratios [19,20], which, though not as precise or consistent between separate experiments as we would have liked them to be, have nevertheless reached a level where they are accurate enough to begin to constrain the mUED model [21]. These constraints form the subject of the present study.

Before we go on to actually study the Higgs boson decay widths, however, it may be noted that bounds on the size parameter $R^{-1}$ quoted from hadron collider studies [22] are generally based on expanded spectra arising when we sum KK levels up to $N = 20$ or even $N = 40$, which, as we have shown, is incompatible with stability of the electroweak vacuum. *We should set aside such hadron collider bounds on the mUED model.* The LEP bound $R^{-1} > 260$ GeV, obtained at $3\sigma$ from precision electroweak tests [23], may, however, be taken as a certainty. In a recent work [24], it has been shown that even if we sum up to five KK levels, a lower bound of $R^{-1} > 720$ GeV at 95% C.L. can be obtained by noting the nonobservation by the CMS Collaboration of dilepton signals [25] arising from the decay of $n = 2$ resonances of the mUED model in the 7–8 TeV runs of the LHC. The purpose of the present study is, therefore, to ascertain if the existing data on the Higgs boson decay channels can provide even better constraints.

Turning then, to the Higgs boson decays, the actual experimentally measured quantities are the so-called *signal strengths* [19,20]. For a decay $H \rightarrow X\bar{X}$, the signal strength is defined by



FIG. 1 (color online). Variation of $\Lambda/R^{-1}$, where $\Lambda$ is the cutoff induced by destabilization of the electroweak vacuum, as a function of size parameter $R^{-1}$. The (red) hatched band represents variations in the Higgs boson mass from 122 to 127 GeV, and horizontal (blue) lines represent KK levels.

TABLE I.  ATLAS [19] and CMS [20] data on Higgs boson signal strengths, as reported in the summer of 2013. For $\mu_{\tau\tau}$ we use the March 2013 results of ATLAS [26].

|       | $\mu_{WW}$ | $\mu_{ZZ}$ | $\mu_{\tau\tau}$ | $\mu_{\gamma\gamma}$ |
|-------|------------|------------|------------------|----------------------|
| ATLAS | $0.99^{+0.31}_{-0.28}$ | $1.43^{+0.40}_{-0.35}$ | $0.8 \pm 0.7$ | $1.55^{+0.33}_{-0.28}$ |
| CMS   | $0.68 \pm 0.20$ | $0.92 \pm 0.28$ | $1.10 \pm 0.41$ | $0.77 \pm 0.27$ |

$$\mu_{X\bar{X}} = \frac{\sigma(pp \to H^0) \times \mathcal{B}(H^0 \to X\bar{X})}{\sigma^{(\mathrm{SM})}(pp \to H^0) \times \mathcal{B}^{(\mathrm{SM})}(H^0 \to X\bar{X})}, \quad (1)$$

where $\mathcal{B}(H^0 \to X\bar{X})$ is the branching ratio of the Higgs boson to an $X\bar{X}$ pair, and $\sigma(pp \to H^0)$ is the cross section for single Higgs production at the LHC. The superscript (SM) denotes the SM prediction. Obviously, if the SM is the correct theory, then the experimental data will eventually converge on the results $\mu_{X\bar{X}} \simeq 1$ for all the channels $X$. On the other hand, deviations from unity will indicate new physics. As of now, the ATLAS and CMS Collaborations at CERN have measured signal strengths for $X\bar{X} = WW^*$, $ZZ^*$, $b\bar{b}$, $\tau^-\tau^+$, $\gamma\gamma$. Of these, the case $X\bar{X} = b\bar{b}$ is not very viable yet because of large errors. The other four have been measured with a better degree of precision. The results are given in Table I below.

We now discuss how to predict the values of $\mu_{X\bar{X}}$ in the mUED model. Using the fact that the parton-level cross section for gluon fusion $gg \to H^0$ is related to the decay width of $H^- \to gg$ by the linear relation

$$\sigma(gg \to H^0) = \frac{\pi^2}{8M_H^3}\Gamma(H^0 \to gg), \quad (2)$$

we can rewrite the signal strength entirely in terms of decay widths as

$$\mu_{X\bar{X}} = \frac{\Gamma(H^0 \to gg)}{\Gamma^{(\mathrm{SM})}(H^0 \to gg)} \times \frac{\Gamma(H^0 \to X\bar{X})}{\Gamma^{(\mathrm{SM})}(H^0 \to X\bar{X})} \times \frac{\Gamma_H^{(\mathrm{SM})}}{\Gamma_H}, \quad (3)$$

where

$$\Gamma_H = \sum_X \Gamma(H^0 \to X\bar{X}) \quad (4)$$

and all parton density function-related effects (to leading order) in the cross section may be expected to cancel in the ratio. All we have to do, therefore, is to calculate the decay widths of the Higgs boson in the mUED model and the SM, and take the appropriate ratios. All the formulas relevant for these are available in the literature, but, for the sake of completeness and having a consistent notation, we list the most important formulas below.

In the SM, the decay width of the Higgs boson to a pair of leptons is given by [27]

$$\Gamma(H^0 \to \ell^+\ell^-) = \frac{\alpha(M_H)}{8\sin^2\theta_W}\frac{m_\ell^2}{M_W^2}M_H\left(1 - \frac{4m_\ell^2}{M_H^2}\right)^{3/2}, \quad (5)$$

where $\alpha(Q)$ is the running QED coupling at the mass scale $Q$. The corresponding decay width to a pair of quarks is given by [27]

$$\Gamma(H^0 \to q\bar{q}) = \frac{3\alpha(M_H)}{8\sin^2\theta_W}\frac{m_q^2(M_H)}{M_W^2}M_H\left(1 - \frac{4m_q^2}{M_H^2}\right)^{3/2}$$
$$\times \left\{1 + 5.67\frac{\alpha_s(M_H)}{\pi}\right\}, \quad (6)$$

where the last factor represents the QCD corrections to the decay width [28], and the running quark mass is given by [29]

$$m_q^2(M_H) = m_q^2\left\{\frac{\alpha_s(M_H)}{\alpha_s(m_q)}\right\}^{24/23}, \quad (7)$$

where $\alpha_s(Q)$ is the running QCD coupling at the mass scale $Q$.

The SM decay width of the Higgs boson to a $WW^*$ pair is given by [30]

$$\Gamma(H^0 \to WW^*) = \frac{3\alpha^2(M_H)}{32\pi\sin^4\theta_W M_H}F(M_W) \quad (8)$$

and that to a $ZZ^*$ pair by [30]

$$\Gamma(H^0 \to ZZ^*) = \frac{\alpha^2(M_H)}{72\pi\sin^4 2\theta_W M_H}$$
$$\times (63 - 120\sin^2\theta_W + 160\sin^4\theta_W)F(M_Z), \quad (9)$$

where

$$F(M) = -\frac{1}{2}\left(1 - \frac{M^2}{M_H^2}\right)\left(47M^2 - 13M_H^2 + \frac{2M_H^4}{M^2}\right)$$
$$- 3\left(M_H^2 - 6M^2 + \frac{4M^4}{M_H^2}\right)\ln\frac{M^2}{M_H^2}$$
$$+ 3\left(M_H^2 - 8M^2 + \frac{20M^4}{M_H^2}\right)$$
$$\times \frac{M_H}{\sqrt{4M^2 - M_H^2}}\cos^{-1}\frac{M_H}{2M}\left(3 - \frac{M_H^2}{M^2}\right). \quad (10)$$

It is important to note that QCD corrections are significant only in the decay widths of the Higgs boson to quarks and can be neglected for all other decay modes. Likewise, the mUED contributions to the above decay modes are negligible, arising, as they do, from higher order effects which

are severely suppressed by the heavy masses of the KK modes.

The decay modes which will be of most interest in the present work are, however, those that occur at the one-loop level in the SM, viz. the decays of the Higgs boson to a pair of gluons ($H^0 \to gg$) or a pair of photons ($H^0 \to \gamma\gamma$). Formulas for the partial decay widths in the SM are given in Ref. [27], and the extra contributions in the mUED, which occur at the same level in perturbation theory, are given in Ref. [31]. We list, below, these formulas in a common notation, with a couple of modifications to the formulas of Ref. [31], which will be mentioned at the appropriate juncture.

The partial decay width of the Higgs boson to a pair of gluons is given by

$$
\Gamma(H^0 \to gg) = \frac{\alpha(M_H)\alpha_s^2(M_H)}{72\pi^2 \sin^2\theta_W} \frac{1}{M_H^5 M_W^2} |\Omega_{gg}^{(SM)} + \Omega_{gg}^{(KK)}|^2
$$
$$
\times \left\{ 1 + 17.92 \frac{\alpha_s(M_H)}{\pi} + 156.8 \frac{\alpha_s^2(M_H)}{\pi^2} \right.
$$
$$
\left. + 467.7 \frac{\alpha_s^3(M_H)}{\pi^3} \right\},  \qquad (11)
$$

where the expression in braces indicates the QCD corrections [28] and the loop integral functions are given by

$$
\Omega_{gg}^{(SM)} = \sum_q 3m_q^2\{2M_H^2 - (M_H^2 - 4m_q^2)f(m_q)\},
$$

$$
\Omega_{gg}^{(KK)} = \sum_q \sum_{n=1}^{N} 3m_q^2 \{4M_H^2 - (M_H^2 - 4m_{q,n,1}^2)
$$
$$
\times f(m_{q,n,1}) - (M_H^2 - 4m_{q,n,2}^2)f(m_{q,n,2})\}, \qquad (12)
$$

where $m_{q,n,1}$ and $m_{q,n,2}$ are the two eigenvalues of the mass matrix

$$
\mathcal{M}_q^{(n)} = \begin{pmatrix} m_{qL}^{(n)} & m_q \\ m_q & -m_{qR}^{(n)} \end{pmatrix} \qquad (13)
$$

for the $n$th-level KK modes of the quarks, where

$$
[m_{qL}^{(n)}]^2 = \frac{n^2}{R^2} + m_q^2 + \delta_{qL}^{(n)}, \qquad [m_{qR}^{(n)}]^2 = \frac{n^2}{R^2} + m_q^2 + \delta_{qR}^{(n)}
$$
$$
(14)
$$

in terms of the radiative corrections $\delta_{qL}^{(n)}$ and $\delta_{qR}^{(n)}$, which are given by [13]

$$
\delta_{qL}^{(n)} = \frac{n}{4\pi R}\left( 6\alpha_s + \frac{27\alpha}{8\sin^2\theta_W} + \frac{\alpha}{8\cos^2\theta_W} - \frac{3y_q^2}{2}\right) \ln\frac{\Lambda R}{n},
$$
$$
\delta_{uR}^{(n)} = \frac{n}{4\pi R}\left( 6\alpha_s + \frac{2\alpha}{\cos^2\theta_W} - 3y_u^2 \right) \ln\frac{\Lambda R}{n},
$$
$$
\delta_{dR}^{(n)} = \frac{n}{4\pi R}\left( 6\alpha_s + \frac{\alpha}{2\cos^2\theta_W} - 3y_d^2 \right) \ln\frac{\Lambda R}{n} \qquad (15)
$$

with the coupling constants being evaluated at the scale $n/R$. The function $f(m)$ is the usual loop integral [27]

$$
f(m) = \begin{cases} -2\left(\sin^{-1}\frac{M_H}{2m}\right)^2 & \text{for } m > \frac{M_H}{2}, \\ -\frac{\pi^2}{2} & \text{for } m = \frac{M_H}{2}, \quad (16) \\ \frac{1}{2}\left(\ln\frac{M_H + \sqrt{M_H^2 - 4m^2}}{M_H - \sqrt{M_H^2 - 4m^2}} - i\pi\right)^2 & \text{for } m < \frac{M_H}{2}. \end{cases}
$$

In using these formulas, we differ from Ref. [31] in two ways:

(1) we consider the sum over KK modes to terminate at $N$, which is the largest integer smaller than $\Lambda R$ as given in Fig. 1, instead of summing to infinity, as was done in Ref. [31]; and

(2) we consider the splitting between mass eigenstates of KK modes of quarks at the level $n$, whereas Ref. [31] assumed them to be degenerate. Of course, the fact that the off-diagonal terms in the mass matrix of Eq. (13) are $m_q$ indicates that such splitting between these states as does occur will be perceptible only in the third generation.

In a similar vein, the partial decay width of the Higgs boson to a pair of photons is given by

$$
\Gamma(H^0 \to \gamma\gamma) = \frac{\alpha^3(M_H)}{16\pi^2 \sin^2\theta_W} \frac{1}{M_H^5 M_W^2} |\Omega_{\gamma\gamma}^{(SM)} + \Omega_{\gamma\gamma}^{(KK)}|^2,
$$
$$
(17)
$$

where the loop integral functions are given by

$$
\Omega_{\gamma\gamma}^{(SM)} = \sum_q e_q^2 \omega_q^{(SM)} + \sum_\ell e_\ell^2 \omega_\ell^{(SM)} + \omega_W^{(SM)},
$$

$$
\Omega_{\gamma\gamma}^{(KK)} = \sum_{n=1}^{N}\left[ \sum_q e_q^2 \omega_q^{(n)} + \sum_\ell e_\ell^2 \omega_\ell^{(n)} + \omega_W^{(n)} \right] \qquad (18)
$$

in terms of [27]

$$
\omega_q^{(SM)} = 3m_q^2\{2M_H^2 - (M_H^2 - 4m_q^2)f(m_q)\},
$$
$$
\omega_\ell^{(SM)} = m_\ell^2\{2M_H^2 - (M_H^2 - 4m_\ell^2)f(m_\ell)\},
$$
$$
\omega_W^{(SM)} = -3M_W^2\{M_H^2 - (M_H^2 - 2M_W^2)f(M_W)\} - \frac{1}{2}M_H^4
$$
$$
(19)
$$

and [31]

$$\omega_q^{(n)} = 3m_q^2\{4M_H^2 - (M_H^2 - 4m_{q,n,1}^2)f(m_{q,n,1}) - (M_H^2 - 4m_{q,n,2}^2)f(m_{q,n,2}^2)\},$$

$$\omega_\ell^{(n)} = m_\ell^2\{4M_H^2 - (M_H^2 - 4m_{\ell,n,1}^2)f(m_{\ell,n,1}) - (M_H^2 - 4m_{\ell,n,2}^2)f(m_{\ell,n,2}^2)\},$$

$$\omega_W^{(n)} = -4M_W^2 M_H^2 + \{4M_W^2(M_H^2 - 2M_{W,n}^2) - M_{W,n}^2 M_H^2\}f(M_{W,n}) - \frac{1}{2}M_H^4, \tag{20}$$

where the lepton mass eigenvalues $m_{\ell,n,1}$ and $m_{\ell,n,2}$ are, for all practical purposes, degenerate.

Using these formulas, we can now find the signal strengths predicted in the mUED model as a function of the size parameter. To understand this behavior, let us note the conclusions of Ref. [31], which remain qualitatively— though not quantitatively—true in our analysis as well. These may be summed up as follows.

(i) The tree-level decay widths of the Higgs boson are practically the same in the SM and the mUED model.

(ii) The decay width of the Higgs boson to a pair of gluons is considerably enhanced in the mUED model, especially when $R$ is taken close to its lower experimental bound (see Fig. 2).

(iii) The decay width of the Higgs boson to a pair of photons is suppressed in the mUED model, especially when $R$ is taken close to its lower experimental bound (see Fig. 2).

In our analysis, we obtain numerically different results from Ref. [31] because of two reasons. In the first place, we note that the sum over KK modes in our case is truncated at values of $n$ between 3 and 5, whereas Ref. [31] took the sum to infinity. As a result, we obtain significantly smaller mUED contributions. The second point is that because of this low cutoff, we are able to take $R^{-1}$ somewhat lower than what the earlier collider-based bounds permit us, and
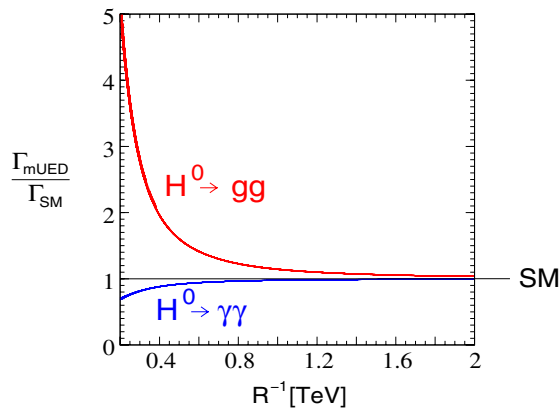
these lower values could then lead to larger mUED contributions.

If we take a closer look at Eq. (3), however, we see that there are more conflicting effects. The three channels with $X\bar{X} = WW^*$, $ZZ^*$ and $\tau\tau$ will all receive enhancements in the mUED model through the first factor on the right of Eq. (3). The second factor will be practically unity, as we have explained above. The third factor, however, will suppress the signal strength if there are large enough mUED contributions in the first factor. Owing to these opposed effects, the enhancement in signal strength is not as large as it might have been otherwise.

A curious fact worth noting is that the variation in the last factor arises only because we do not yet have an accurate measurement of the total decay width of the Higgs boson. If the Higgs boson decay width could be accurately determined from a line shape analysis, as was done for the $W$ and $Z$ bosons at LEP and Tevatron, then that result alone could have been used to constrain any new physics model. In the case of the $\gamma\gamma$ channel, the second factor on the right of Eq. (3) will be somewhat smaller than unity, as a result of which the signal strength will be somewhat more suppressed than in the other cases. It is therefore difficult, in the mUED model, to predict large excesses in the partial width of $H^0 \to \gamma\gamma$. We reiterate, therefore, that the mUED enhancement in $H^0 \to gg$ and the suppression of $H^0 \to \gamma\gamma$ are both in agreement with the results of Ref. [31], though the actual deviations are much more modest in the present case—a consequence of the small number of KK modes which contribute to these deviations.

These diverse effects together contribute to the numerical results exhibited in Fig. 3. The four panels in this figure correspond to the four decays $H^0 \to WW^*$, $ZZ^*$, $\tau^+\tau^-$ and $\gamma\gamma$, as marked on each respective panel. The solid (black) lines represent the mUED predictions, and, as expected, these fall rapidly to the SM expectation $\mu_{X\bar{X}} = 1$ as $R^{-1}$ increases, in every case. The thickness of these lines indicates the effect of varying $M_H = 122$–$127$ GeV. It is clear from the figure that this is not a very significant effect.[1] In fact, the solid (black) curves for $\mu_{WW}$, $\mu_{ZZ}$ and $\mu_{\tau\tau}$ are identical, since the only effect of introducing mUED lies in the first and last factors of Eq. (3), which depend



FIG. 2 (color online).   Illustrating the effect of KK modes on the partial decay widths of $H^0 \to gg$ and $H^0 \to \gamma\gamma$. The former is always enhanced, while the latter is always suppressed, compared to the SM prediction.

---

[1]The effect of varying the top quark Yukawa coupling is subleading to this variation, which is why we do not show it at all in the present work.

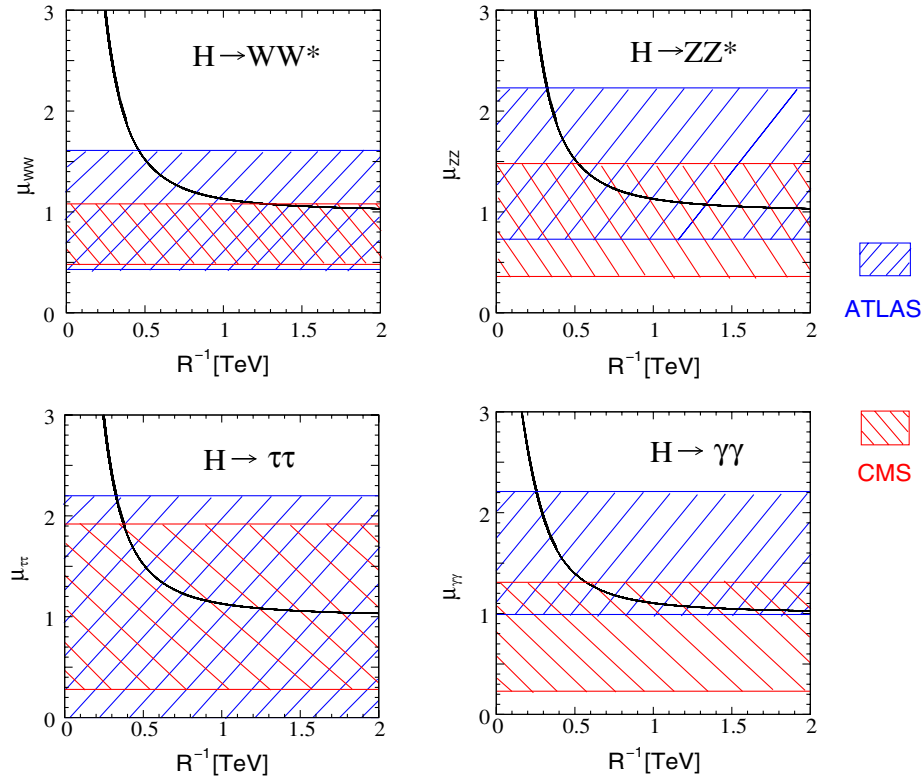FIG. 3 (color online).   Illustrating the variation with $R^{-1}$ of the signal strengths $\mu_{WW}$, $\mu_{ZZ}$, $\mu_{\tau\tau}$ and $\mu_{\gamma\gamma}$, as marked on the respective panels. The solid (black) lines show the mUED prediction, with their thickness representing the effect of varying the Higgs boson mass $M_H$ from 122 to 127 GeV. The oppositely hatched regions (blue and red) denote, as indicated in the key on the right, the 95% C.L. limits from the ATLAS and CMS Collaborations, respectively, quoted in Table I.

mainly on $\Gamma(H^0 \to gg)$. The solid (black) curve for $\mu_{\gamma\gamma}$ is clearly different, as one would expect. However, the reason for showing each signal strength separately lies in the fact that the experimental constraints are significantly different in each of these channels. For both the ATLAS and CMS data, the strongest constraints come, in fact, from the $WW^*$ channel. For a 125–126 GeV Higgs boson, these come out as $R^{-1} > 463$ GeV (1.3 TeV) for the ATLAS (CMS) results, which are far more restrictive than anything we can get from precision tests, and—at least for the CMS data —surpass the bounds from dilepton channels [24] by a factor close to 2.

The 95% C.L. constraints from the other channels are illustrated, together with the $WW^*$ channel, in Fig. 4, in the form of a bar graph. It is apparent, even from Fig. 3, that the CMS data provide significantly stronger constraints, at this level, than the ATLAS data. In particular, if we consider the ATLAS data for $H^0 \to \gamma\gamma$, where there appears to be an excess at the $1\sigma$ level over the SM prediction, this appears to hint at lower values of $R^{-1}$, though—as the graph shows —large values of $R^{-1}$ are perfectly consistent with the 95% C.L. limits. In view of the substantial differences between the two experimental results, it may be premature to read too much into these constraints, but it is clear that for the $WW^*$ channel, at least, we do find a reasonable level

of consistency. Since this is the channel which provides the most stringent bounds on $R^{-1}$, these are perhaps the most acceptable among the four sets of constraints, at least at the present time.

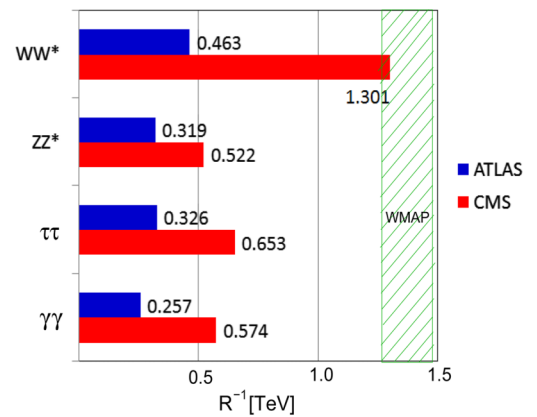In Fig. 4, as mentioned above, we have shown a bar graph illustrating the individual 95% C.L. constraints on



FIG. 4 (color online).   The 95% C.L. lower bounds (in TeV) on the size parameter $R^{-1}$ arising from four different Higgs boson decay channels. Numbers juxtaposed with the bars are the numerical value of the bounds. The hatched region is the WMAP-compatible region as reported in Ref. [32].

$R^{-1}$ from each of these four channels. The upper (blue) and lower (red) bars represent bounds arising from the ATLAS and CMS data, respectively. For the ATLAS data, the strongest constraint is from the $WW^*$ channel, but even the $ZZ^*$ and $\tau\tau$ channels are more restrictive than the LEP constraints. So far as the ATLAS data are concerned, obviously no useful constraint can be expected to arise from the $\gamma\gamma$ channel, but if the excess in this channel turns out to be a genuine feature, it will favor the mUED model (among other rival models) with a somewhat smaller value of $R^{-1}$. The CMS data, on the other hand, are much more restrictive. While the $WW^*$ channel pushes the lower bound to as high as 1.3 TeV, none of the other channels permit a value of $R^{-1}$ as low as 500 GeV, which is a substantial improvement over the LEP bound of 260 GeV but is not as restrictive as the dilepton bound obtained in Ref. [24].

At this point it is interesting to ask whether the mUED model, with the above constraints, is compatible with the relic density of dark matter as obtained from the Wilkinson Microwave Anisotropy Probe (WMAP) analysis of the cosmic microwave background radiation. For, after all, the most important phenomenological motivation for a UED model is that it provides a natural dark matter candidate: it follows that this model should be able to explain the dark matter relic density $\Omega_d h^2 = 0.1120 \pm 0.0056$ as reported by the WMAP Collaboration. The most complete analysis of this has been carried out in Ref. [32], taking into account all possible decay and coannihilation channels at the one-loop level and including $n = 2$ Kaluza-Klein states. The range of $R^{-1}$ allowed in this model at 95% C.L. comes out to be $1.37 \pm 0.11$ TeV, which appears in Fig. 4 as the (green) hatched region to the extreme right of the graphic. It is interesting to see that the strongest constraint obtained from the Higgs boson signal strengths barely impinges upon the left end of this region, showing that the mUED model is still compatible with the observed relic density of dark matter.

There are a couple of caveats to the above conclusion, however. The pre-Higgs discovery results of Ref. [32] were obtained using $M_H = 120$ GeV and summing over 20 Kaluza-Klein levels, i.e. setting $\Lambda R = 20$. Both of these require to be updated to $M_H \simeq 125.5$ GeV and $\Lambda R \leq 5$, as used in the present work. The first change may not be very significant, so far as the dark matter is concerned, but the second will definitely lead to a more compressed mUED spectrum for $n = 1, 2$ states, and this, in turn, will cause the coannihilation rates to rise. The detailed analysis of this is beyond the scope of the present work, but one can make an educated guess that a small rise in the coannihilation rates would push the WMAP-allowed region in $R^{-1}$ to somewhat lower values, shifting, say, by about 50 GeV. This would then combine with the lower bound obtained here to give a narrow window of about 100 GeV where the mUED model is consistent with all the constraints.

TABLE II. The $3\sigma$ lower bounds (in GeV) on $R^{-1}$ using the ATLAS and CMS data from Table I and the signal strengths from Fig. 3.

| | $\mu_{WW}$ | $\mu_{ZZ}$ | $\mu_{\tau\tau}$ | $\mu_{\gamma\gamma}$ |
|---|---|---|---|---|
| ATLAS | 369 | 278 | 248 | 207 |
| CMS | 685 | 413 | 306 | 402 |

The lower bound of $R^{-1} > 1.3$ TeV obtained from our computations represents a very strong constraint for the mUED model and would severely impact the direct searches planned for the 14 TeV run of the LHC. It is interesting, therefore, to ask how far these bounds can be relaxed if we consider the ATLAS and CMS data at the $3\sigma$ level rather than at 95% confidence level. These bounds are presented in Table II below, and are naturally weaker, with the strongest bound lying at $R^{-1} > 685$ GeV, which is still a significant improvement over the precision tests.[2]

If we further relax the constraints to the $5\sigma$ level, we find that the $WW^*$ channel data imply bounds on $R^{-1} > 280(432)$ GeV from the ATLAS (CMS) data. Even with this very loose constraint, the lower bound of 432 GeV from the CMS data is still stronger than the LEP constraint. However, if we go by the conventional wisdom that $2\sigma$ deviations constitute a hint, $3\sigma$ deviations—or the lack thereof—constitute a bound, and $5\sigma$ is required for a discovery, then the stronger constraint $R^{-1} > 1.3$ TeV may be quite credible.

It is amusing to speculate on how these bounds might improve in the 14 TeV run of the LHC—under the somewhat pessimistic assumption that no deviations from the SM will be discovered. Estimates [33] of the cross section for $pp \rightarrow H^0$ at 8 and 14 TeV indicate an enhancement in the cross section by a factor around 2.5. Assuming that the integrated luminosity in the 14 TeV run will be as high as 1.5 ab$^{-1}$, this represents an enhancement of 100 times over the statistics collected at 8 TeV. Thus, the number of Higgs boson events in the 14 TeV run will be around 250 times the number collected at the 8 TeV run. If we concentrate on the $WW^*$ signal and assume that the errors will scale as the inverse square root of the number of Higgs boson decay events, then the error on the CMS measurement of $\mu_{WW}$ could go down as low as 0.012. This is certainly an overestimate, since it does not take into account systematic effects, but it is probably safe to assume [34] that the error could be as low as 5%. Assuming, therefore, that we have a measured value $\mu_{WW} = 1.00 \pm 0.05$ (from either experiment, or from both combined), we immediately predict a 95% C.L. limit $R^{-1} > 1.58$ TeV, which would increase to 1.90 TeV if the integrated luminosity is doubled to 3 ab$^{-1}$. For such large values of

---

[2]This is also definitely stronger than the $3\sigma$ bounds obtainable from dilepton signals, which would certainly lie around 600 GeV or below, if we go by the results quoted in Fig. 4 of Ref. [24].

$R^{-1}$, it is more or less sure that direct searches for mUED signals will fail, and the LKP will surely become too heavy to explain the observed relic density of dark matter. In this admittedly pessimistic scenario, there would be no real motivation to study the mUED model any further.

Of course, we do not have any compelling reason to think that the above scenario is a true picture of the future. In fact, given the urgency with which an explanation of the composition of dark matter is required, we may well hope for just the reverse of this scenario, i.e. the observation of deviations in some of the Higgs boson partial decay widths in the 14 TeV run. In that case, we can reverse some of the arguments of the present study to show that a mUED explanation of such a deviation would be immediately available for some value of $R^{-1}$ in the range of 1–2 TeV.

To sum up, then, we have studied constraints on the mUED model from the measured Higgs boson signal strengths in the decays $H^0 \rightarrow WW^*$, $ZZ^*$, $\tau\tau$ and $\gamma\gamma$ channels. The mUED calculations have been carried out carefully, taking into account the fact that this model has a very low cutoff due to vacuum stability arguments. Even with the reduced effects due to this low cutoff, however, we find that the present CMS data can push the lower bound on the size parameter $R^{-1}$ of this model as high as 1.3 TeV at 95% C.L. (or 685 GeV at $3\sigma$). ATLAS data are less

restrictive, but in any case, do serve to push the value of $R^{-1}$ above about 500 GeV. All this represents an enormous improvement over the $3\sigma$ bound of around 260 GeV arising from precision electroweak tests at the LEP collider, as well as a factor close to 2 greater than the 95% dilepton bounds obtained from the early runs of the LHC. We then go on to argue that these signal strengths can be used to probe the mUED model up to $R^{-1} \approx 2$ TeV in the 14 TeV run of the LHC. Such searches will fully explore the WMAP-allowed region in the parameter space, assuming that the LKP is the dominant component of the observed dark matter density of the Universe.

[1] ATLAS Collaboration, Phys. Lett. B **716**, 1 (2012); CMS Collaboration, Phys. Lett. B **716**, 30 (2012); TEVNPH Working Group (for the CDF and D0 Collaborations), Fermilab Report No. FERMILAB-CONF-12-318-E, 2012.

[2] S. Dimopoulos and L. Susskind, Nucl. Phys. **B155**, 237 (1979); E. Eichten and K. D. Lane, Phys. Lett. B **90**, 125 (1980); C. Csaki, C. Grojean, H. Murayama, L. Pilo, and J. Terning, Phys. Rev. D **69**, 055006 (2004).

[3] B. W. Lee, C. Quigg, and H. B. Thacker, Phys. Rev. D **16**, 1519 (1977).

[4] W. J. Marciano, G. Valencia, and S. Willenbrock, Phys. Rev. D **40**, 1725 (1989); C. F. Kolda and H. Murayama, J. High Energy Phys. 07 (2000) 035.

[5] See M. Sher, Phys. Rep. **179**, 273 (1989), and references therein, for early work on the subject; for more recent work, see J. Ellis, J. R. Espinosa, G. F. Giudice, A. Hoecker, and A. Riotto, Phys. Lett. B **679**, 369 (2009); J. Elias-Miro, J. R. Espinosa, G. F. Giudice, G. Isidori, A. Riotto, and A. Strumia, Phys. Lett. B **709**, 222 (2012); G. Degrassi, S. Di Vita, J. Elias-Miro, J. R. Espinosa, G. F. Giudice, G. Isidori, and A. Strumia, J. High Energy Phys. 08 (2012) 098; F. Bezrukov, M. Y. Kalmykov, B. A. Kniehl, and M. Shaposhnikov, J. High Energy Phys. 10 (2012) 140; M. Holthausen, K. S. Lim, and M. Lindner, J. High Energy Phys. 02 (2012) 037.

[6] S. Alekhin, A. Djouadi, and S. Moch, Phys. Lett. B **716**, 214 (2012).

[7] For a comprehensive discussion, see G. Bertone *et al.*, *Particle Dark Matter: Observations, Models and Searches* (Cambridge University Press, Cambridge, England, 2010).

[8] P. J. E. Peebles and B. Ratra, Rev. Mod. Phys. **75**, 559 (2003).

[9] A. Riotto and M. Trodden, Annu. Rev. Nucl. Part. Sci. **49**, 35 (1999).

[10] See, for example, S. P. Martin, in *A Supersymmetry Primer*, edited by G. L. Kane (World Scientific, Singapore, 2010), p. 1; M. Drees, R. Godbole, and P. Roy, *Theory and Phenomenology of Sparticles* (World Scientific, Hackensack, NJ, 2004); H. Baer and X. Tata, *Weak Scale Supersymmetry* (Cambridge University Press, Cambridge, England, 2006).

[11] T. Appelquist, H. C. Cheng, and B. A. Dobrescu, Phys. Rev. D **64**, 035002 (2001).

[12] D. Hooper and S. Profumo, Phys. Rep. **453**, 29 (2007).

[13] H.-C. Cheng, K. T. Matchev, and M. Schmaltz, Phys. Rev. D **66**, 036005 (2002); A. K. Datta, K. C. Kong, and K. T. Matchev, New J. Phys. **12**, 075017 (2010); B. Bhattacherjee, A. Kundu, S. K. Rai, and S. Raychaudhuri, Phys. Rev. D **81**, 035021 (2010).

[14] A. K. Datta, K. C. Kong, and K. T. Matchev, Phys. Rev. D **72**, 096006 (2005); **72**, 119901(E) (2005); B. Bhattacherjee, M. Guchait, S. Raychaudhuri, and K. Sridhar, Phys. Rev. D **82**, 055006 (2010).

[15] K. R. Dienes, E. Dudas, and T. Gherghetta, Phys. Lett. B **436**, 55 (1998); Nucl. Phys. **B537**, 47 (1999).

[16] G. Bhattacharyya, A. Datta, S. K. Majee, and A. Raychaudhuri, Nucl. Phys. **B760**, 117 (2007).

[17] M. Blennow, H. Melbéus, T. Ohlsson, and H. Zhang, Phys. Lett. B **712**, 419 (2012).

[18] ATLAS Collaboration, Report No. ATLAS-CONF-2013-102, 2013.

[19] ATLAS Collaboration, CERN Report No. CERN-PH-EP-2013-103, 2013.

[20] CMS Collaboration, Report No. CMS-PAS-HIG-13-005, 2013.

[21] G. Bélanger, A. Belyaev, M. Brown, M. Kakizaki, and A. Pukhov, Phys. Rev. D **87**, 016008 (2013); U. K. Dey and T. S. Ray, Phys. Rev. D **88**, 056016 (2013).

[22] T. Kakuda, K. Nishiwaki, K.-y. Oda, and R. Watanabe, Phys. Rev. D **88**, 035007 (2013).

[23] A. Datta and S. Raychaudhuri, Phys. Rev. D **87**, 035018 (2013).

[24] L. Edelhauser, T. Fläcke, and M. Kramer, J. High Energy Phys. 08 (2013) 091.

[25] CMS Collaboration, Report No. CMS-PAS-EXO-12-061, 2012.

[26] ATLAS Collaboration, Report No. ATLAS-CONF-2013-034, 2013.

[27] V. Barger and R. J. N. Phillips, *Collider Physics* (Addison-Wesley, Reading, MA, 1997), 2nd ed.

[28] M. Schreck and M. Steinhauser, Phys. Lett. B **655**, 148 (2007).

[29] J. Beringer *et al.* (Particle Data Group), Phys. Rev. D **86**, 010001 (2012).

[30] W.-Y. Keung and W. J. Marciano, Phys. Rev. D **30**, 248 (1984).

[31] F. J. Petriello, J. High Energy Phys. 05 (2002) 003; see also A. Datta and S. K. Rai, Int. J. Mod. Phys. A **23**, 519 (2008); S. K. Rai, Int. J. Mod. Phys. A **23**, 823 (2008).

[32] G. Bélanger, M. Kakizaki, and A. Pukhov, J. Cosmol. Astropart. Phys. 02 (2011) 009.

[33] W. Beenakker, R. Hopker, and M. Spira, arXiv:hep-ph/9611232.

[34] See, for example, P. Giacomelli, The Solvay Workshop on 'Facing the Scalar Sector', Brussels, 2013, http://www.solvayinstitutes.be/events/Facing_the_Scalar_Challenge/24_Giacomolli.pdf.